

Quantum Control of Radical Pair Dynamics beyond Time-Local Optimisation

Farhan T. Chowdhury , Matt C. J. Denton , Daniel C. Bonser, and Daniel R. Kattnig 
Department of Physics and Astronomy, University of Exeter, Stocker Road, Exeter EX4 4QL, UK

By extending Gradient Ascent Pulse Engineering (GRAPE) to allow for optimising reaction yields, we realise arbitrary waveform-based control in spin-selective recombination reactions of radical pairs in the low magnetic field regime. This overcomes drawbacks of previous time-local optimisation approaches for realising reaction control, which were limited in their applicability to radical pairs driven by high biasing fields. We demonstrate how efficient time-global optimisation of the radical pair recombination yields can be realised by gradient based methods augmented with time-blocking, sparse sampling of the yield, and evaluation of the central single-timestep propagators and their Fréchet derivatives using iterated Trotter-Suzuki splittings. Results are shown for both a toy model, previously used to demonstrate coherent control of radical pair reactions in the simpler high-field scenario, and furthermore for a realistic exciplex-forming donor-acceptor system comprising 16 nuclear spins. This raises prospects for the spin-control of actual radical pair systems in ambient magnetic fields, by suppressing or boosting radical reaction yields using purpose-specific radio-frequency waveforms, paving the way for radical inspired qubit architectures for reaction-yield-dependent quantum magnetometry and potentially applications of quantum control to biochemical radical pair reactions.

I. INTRODUCTION

The rapidly evolving field of optimal quantum control (OQC) seeks to manipulate phenomena at the quantum scale by devising and implementing perturbations, typically in the form of electromagnetic pulses, to steer a given quantum system to a desired target. Fuelled by demonstrable successes in nuclear magnetic resonance (NMR) [1–3] pulse engineering and the control of ultra-fast excited-state reactions by laser fields [4], pioneering developments in “coherent control” were first conceived in the field of chemistry. Today OQC has developed into a mature discipline that is central to modern quantum technologies associated with the second quantum revolution [5], with numerous applications across quantum information processing and quantum metrology [1]. We here demonstrate the use of a Gradient Ascent Pulse Engineering (GRAPE)-inspired approach for the open-loop control of singlet recombination yields of radical pairs in weak magnetic fields, thereby putting a renewed spotlight on the control of spin-chemical reactions.

Reactions involving the recombination of radical pair intermediates are well-known to depend on spin-degrees of freedom and their dynamics. Specifically, the electronic singlet and triplet states associated with the two unpaired electrons, one in each radical, of the radical pair can undergo coherent inter-conversion as a consequence of symmetry-breaking interactions—in particular, the hyperfine interactions with surrounding magnetic nuclei. As radical pair recombination preserves spin-multiplicity in the absence of strong spin-orbit coupling, provided that the singlet and triplet states exhibit differential chemical reactivity, the radical pair spin dynamics is reflected in the reaction yields realised via the singlet and triplet channels. By coupling to magnetic fields via the Zeeman interaction, radical pairs furthermore acquire sensitivity to static and oscillatory applied magnetic fields. Studies of effects of oscillatory magnetic fields on radical pair reactions have been realised

for chemical model systems and are central to identifying magnetosensitive radical pair reactions in biology [6, 7]. While a majority of model studies looked at magnetic field effects (MFEs) of monochromatic radio-frequency magnetic fields in the presence of a strong biasing field [8], often referred to as reaction yield detected magnetic resonance (RYDMER), some studies have been realised in a weak static field, in particular for exciplex systems [9–13]. Notably, the radical pair mechanism, or variations thereof [14], are also hypothesised to underpin a compass sense in various animals, including migratory songbirds [15]. In this case, the magnetosensitive radical pair is thought to originate from a photo-induced electron transfer reaction in the flavo-protein cryptochrome. Even though the exact nature of the underlying radical pair has remained unclear, the fact that this compass sense is interruptible by weak monochromatic [16] or broad-band radio-frequency [17] magnetic fields strongly supports an underlying spin mediated mechanism. These observations support the prospect of controlling chemical reactions involving radical pairs, possibly in the near future, in the spin biological context, and the challenging low-field regime, provided that an efficient approach to pulse engineering can be developed.

In their recent work, Masuzawa et al. [18, 19] suggested the control of radical pair reactions based on model calculations for a prototypical spin system. They focus on the classical RYDMER scenario, for which the applied electromagnetic field is in resonance with the electronic Zeeman splitting produced by a strong static field, perturbs the singlet-triplet interconversion of the radical pair and thus affects the yield of geminate recombination. Their control approach, based on theory by Sugawara [20], propagates the spin density operator whereby at every moment the control amplitude is chosen such that an optimisation criterion is bound to not decrease. Since the algorithm optimises the controls in a time-local fashion, it is dubbed as *local optimisation*. By construction, the employed algorithm allows optimising the trajectory

of an observable commuting with the time-independent dynamics generator, i.e. the drift Hamiltonian, or alternatively, an arbitrary observable at *one* chosen moment in time (via back-propagation). While the combined population of the singlet (S) and one of the triplet states (T_0) is hence controllable over time in the high-field limit, the more relevant singlet population falls in the second category. Our approach aims overcome ostensible drawbacks of the time-local optimisation approach by permitting time-global optimisation and by focusing on the singlet recombination yield, i.e. the actual experimental observable (rather than S and T_0 -populations over time or the singlet probability at a moment of time). For realising quantum control of radical pair dynamics in a weak static magnetic field, both of these developments are critical.

We deviate from the traditional GRAPE by optimising reaction yields (rather than a fidelity measure defined at a defined moment in time), accounting for asymmetric radical pair recombination, and, following de Fouquieres et al. [21], by using curvature information of the loss function (rather than steepest descent/ascent). We furthermore address a major objection to GRAPE-based reaction control of radical pairs, namely high computational demands, as also voiced by Masuzawa et al. [18], by suggesting a block-optimisation scheme and sparse sampling of the reaction yield to improve the efficiency of the approach while retaining adequate control fidelity.

II. THEORY

A. Radical Pair Spin Dynamics

We consider a system comprising radicals $A^{\bullet-}$ and $B^{\bullet+}$ subject to singlet-triplet interconversion, undergoing spin-selective recombination reactions as per Fig. 1.

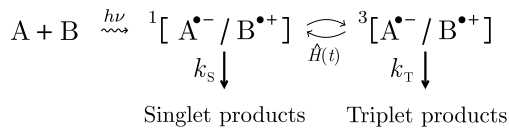


FIG. 1. Reaction Scheme.

The corresponding spin dynamics is described in terms of the time-dependent spin density matrix $\hat{\rho}(t)$ by

$$\frac{d\hat{\rho}(t)}{dt} = -i[\hat{H}(t), \hat{\rho}(t)] - \{\hat{K}, \hat{\rho}(t)\}, \quad (1)$$

with $\hat{H}(t)$ denoting the spin Hamiltonian and

$$\hat{K} = \frac{k_S}{2}\hat{P}_S + \frac{k_T}{2}\hat{P}_T \quad (2)$$

accounting for radical pair recombination. Here, k_S and k_T denote the reaction rate constants in the singlet and triplet state, respectively, and \hat{P}_S, \hat{P}_T are the projection

operators onto the singlet and triplet states. We introduce an effective Hamiltonian given by

$$\hat{A}(T) = \hat{H}(t) - i\hat{K}, \quad (3)$$

allowing us to reformulate eq. (1) as

$$\begin{aligned} \frac{\partial \hat{\rho}(t)}{\partial t} &= -i[\hat{A}(T), \hat{\rho}(t)] \\ &= -i(\hat{A}(T)\hat{\rho} - \hat{\rho}\hat{A}(T)^\dagger), \end{aligned} \quad (4)$$

where $[A, B] = AB - (AB)^\dagger = AB - BA^\dagger \vee B = B^\dagger$. The formal solution to eq. (4) is given by

$$\hat{\rho}(t_n) = \hat{U}(t_n, 0)\hat{\rho}(0)\hat{U}^\dagger(t_n, 0) \quad (5)$$

where the time evolution operator in terms of $\hat{A}(T)$ is

$$\hat{U}(t, 0) = \mathcal{T} \exp \left[-i \int_0^t \hat{A}(\tau) d\tau \right]. \quad (6)$$

Here, \mathcal{T} denotes the time ordering operator, that reorders products of time-dependent operators such that their time arguments decrease going from left to right.

The singlet channel recombination yield is given by

$$Y_S = k_S \int_0^\infty \hat{P}_S(t) dt \quad (7)$$

where $\hat{P}_S(t) = \text{Tr}[\hat{P}_S\hat{\rho}(t)]$ is the survived singlet probability of the radical pair. Note that eq. (4) is of truncated Linblad form (by introducing shelving states, an equivalent formulation in traditional Lindblad form is also possible [22]). Thus, the essentially open quantum system description of radical pair spin dynamics in the presence of spin-selective recombination eq. (1) can be treated in terms of the dynamics of a closed system, albeit with a non-Hermitian dynamics generator, non-unitary evolution operators and non-conserved trace.

Here, we consider radical pairs for which the static part of the Hamiltonian, H_0 , is of the form

$$\hat{H}_0 = \hat{H}_A + \hat{H}_B + \hat{H}_{AB} \quad (8)$$

where $\hat{H}_i, i \in \{A, B\}$ is local to radical i and comprises the Zeeman interaction with the static magnetic field and isotropic hyperfine couplings with surrounding nuclear spins. \hat{H}_{AB} accounts for inter-radical couplings in the form of the exchange interaction. Specifically, each radical is described in terms of corresponding nuclear and electron spin angular momentum operators $\hat{\mathbf{I}}_{ik}$ and $\hat{\mathbf{S}}_i$ by

$$\hat{H}_i = \omega_i \hat{S}_{iz} + \sum_{k=1}^{n_i} \hat{A}_{ik} \hat{\mathbf{I}}_{ik} \cdot \hat{\mathbf{S}}_i. \quad (9)$$

and

$$\hat{H}_{AB} = -j_{ex} \left(2\hat{\mathbf{S}}_A \cdot \hat{\mathbf{S}}_B + \frac{1}{2} \right) \quad (10)$$

where $\omega_i = -\gamma_i B$, with γ_i denoting the gyromagnetic ratio of the electron in radical i and B the applied magnetic field, \hat{A}_{ik} is the isotropic hyperfine coupling constant between electron spin i and the k -th nuclear spin (out of total n_i), and the exchange coupling constant is denoted by j_{ex} . The initial density operator is assumed as

$$\hat{\rho}(0) = \frac{1}{Z_1 Z_2} \hat{P}_S, \quad (11)$$

where $Z_i = \prod_{k=1}^{n_i} (2I_{ik} + 1)$ is the total number of nuclear spin states in radical i and

$$\hat{P}_S = \frac{1}{4} - \hat{\mathbf{S}}_1 \cdot \hat{\mathbf{S}}_2, \quad (12)$$

the singlet projection operator.

B. Gradient-based coherent control

Without loss of generality, we can describe a system undergoing spin dynamics under coherent control with

$$\hat{H}(t) = \hat{H}_0 + \sum_{l=1}^M u_l(t) \hat{V}_l, \quad (13)$$

where \hat{H}_0 is the drift Hamiltonian describing the time-independent part of the system, i.e. the intrinsic radical pair dynamics in the static bias field, as introduced above, $u_l(t)$ are the control amplitudes and \hat{V}_l is the set of control Hamiltonians that couple the controls to the system, for example via the Zeeman interaction. The goal of OQC is to minimise some control objective functional $G[\{u_l(t)\}]$, with a control target subject to physical constraints and other criteria. For our purposes, we focus on minimising the singlet recombination yield of the radical pair, i.e. $G = Y_S$. However, the approach is easily generalised to focus on other reaction outcomes, e.g. accumulated nuclear polarisation. Significant prior work has been concentrated on optimising G subject to the assumption that the values taken by the controls over time may be parameterised by piecewise constant control amplitudes in the time domain [23]. This paradigm, which is central to GRAPE as the first widely applied quantum control algorithm [24], is well aligned with the practical aspect of controlling radical pairs, as standard arbitrary waveform generator (AWG) based control schemes represent pulse inputs as piecewise constant functions. We thus discretise the time axis, $t_0 = 0 < t_1 < t_2 < \dots < t_N = t_{max}$ and we set

$$\hat{H}(t) \approx \hat{H}_0 + \sum_{l=1}^M \sum_{n=1}^N u_{l,n} \chi_n(t) \hat{V}_l \quad (14)$$

with constants $u_{l,n}$ and the indicator function $\chi_n(t)$ defined such that $\chi_n(t) = \begin{cases} 1 & \text{for } t_{n-1} \leq t < t_n \\ 0 & \text{otherwise.} \end{cases}$

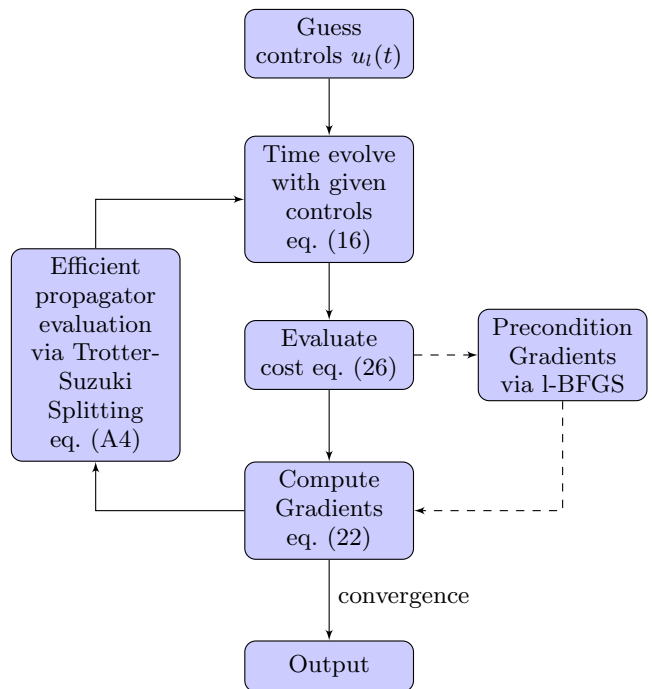


FIG. 2. A simplified flowchart for GRAPE. Initially, the control variables are guessed, and the system is time evolved. The cost is then computed in terms of an objective function, and we get an output where convergence is achieved. Otherwise, exact or approximate gradients with respect to control variables are computed, utilising iteratively accumulated curvature information to update the latter, using which the system is again time evolved and the process repeats.

The corresponding propagators $\hat{U}(t_n, 0)$ are discretised on the temporal grid such that

$$\hat{U}(t_n, 0) = \mathcal{T} \prod_{i=1}^n \hat{U}_i = \hat{U}_n \dots \hat{U}_1 \quad (15)$$

where

$$\hat{U}_i = e^{-i\hat{A}_i \Delta t_i} \quad (16)$$

with $\Delta t_i = t_i - t_{i-1}$ and $\hat{A}_i = \hat{A}(t_{i-1})$. The gradients of G depend on the propagator derivatives, evaluated as

$$\frac{\partial \hat{U}_i}{\partial u_{l,j}} = \delta_{i,j} L_{i,l} = \delta_{i,j} L(i\hat{A}_i \Delta t_i, i\hat{V}_l \Delta t_i) \quad (17)$$

where $L(X, E)$ is the Fréchet derivative of the matrix exponent defined, for every E , by

$$e^{(X+E)} - e^X = L(X, E) + o(\|E\|). \quad (18)$$

More explicitly, we have [25]

$$\begin{aligned} L(X, E) &= \int_0^1 e^{X(1-s)} E e^{Xs} ds \\ &= \sum_{n=1}^{\infty} \frac{1}{n!} \sum_{j=1}^n X^{j-1} E X^{n-j}, \end{aligned} \quad (19)$$

which also allows us to demonstrate that

$$\begin{aligned}\frac{\partial \hat{U}_i^\dagger}{\partial u_{i,j}} &= \delta_{i,j} L(+i\hat{A}_i^\dagger \Delta t_i; +i\hat{V}_i \Delta t_i) \\ &= \delta_{i,j} L^\dagger(-i\hat{A}_i \Delta t_i; -i\hat{V}_i \Delta t_i) \\ &= \delta_{i,j} L_{i,l}^\dagger\end{aligned}\quad (20)$$

Combining the above equations, the gradient of the survived singlet probability,

$$\hat{P}_S(t_n) = \text{Tr}[\hat{P}_S \hat{U}(t_n, 0) \hat{\rho}(0) \hat{U}^\dagger(t_n, 0)], \quad (21)$$

for $k \leq n$, is thus

$$\begin{aligned}\frac{\partial \hat{P}_S}{\partial u_{i,k}} &= -i \text{Tr}(\hat{P}_S \hat{U}_+ [[\hat{W}_{k,l}, \hat{U}_- \hat{\rho}_0 \hat{U}_-^\dagger]] \hat{U}_+^\dagger) \\ &= -i \text{Tr}(\hat{U}_+^\dagger \hat{P}_S \hat{U}_+ [[\hat{W}_{k,l}, \hat{U}_- \hat{\rho}_0 \hat{U}_-^\dagger]]) \\ &= 2\Im[\text{Tr}(\hat{U}_+^\dagger \hat{P}_S \hat{U}_+ \hat{W}_{k,l} \hat{U}_- \hat{\rho}_0 \hat{U}_-^\dagger)] \\ &= 2\Im[\text{Tr}(\hat{P}_S \hat{U}_+ \hat{W}_{k,l} \hat{U}_- \hat{\rho}_0 \hat{U}_+^\dagger)]\end{aligned}\quad (22)$$

where $\hat{W}_{i,l} = i\hat{U}_i^{-1} L_{i,l}$ and

$$\hat{U}_+ = \mathcal{T} \prod_{m=k}^n \hat{U}_m \quad (23)$$

$$\hat{U}_- = \mathcal{T} \prod_{m=1}^{k-1} \hat{U}_m. \quad (24)$$

For $k > n$, the gradient obviously vanishes. In the original formulation of GRAPE, a first-order approximation of $L_{k,l}$ was used [24], which is obtained with $\hat{W}_{i,l} = \hat{V}_l$. For our approach, we use the full Fréchet derivative. Finally, this allows us to approximate the singlet yield by

$$\begin{aligned}Y_S &= k_S \int_0^\infty \hat{P}_S(t) dt \\ &\approx k_S \sum_{n=0}^N w_n \hat{P}_S(t_n)\end{aligned}\quad (25)$$

with w_n denoting suitably chose quadrature weights. The gradient of the singlet yield is then obtained as

$$\frac{\partial Y_S}{\partial u_{i,k}} \approx k_S \sum_{n=k}^N w_n \frac{\partial \hat{P}_S}{\partial u_{i,k}}. \quad (26)$$

III. RESULTS

The control of reaction yields via numerical approaches is expected to be computational costly, which is why Masuzawa et al. [18] had dismissed GRAPE in favour of time-local optimisation in their earlier attempt at realising radical pair-reaction control. The computational demand is particularly large if, as we do here (and unlike [18, 19]), the goal is to optimise yields, which are time-integral quantities (cf. eq. (7)), unlike the typical fidelity

measures in quantum control applications pertaining to the implementation of a state transfer or a unitary operation for a fixed time t . Our approach requires computing N single-time-step propagators alongside their Fréchet derivatives with respect to L control Hamiltonians, and scores of repeated matrix multiplications for evaluating the time-dependent singlet-probabilities and associated gradients, which sum to the recombination yield and its associated gradients. In the Appendix we evaluate the number of required matrix multiplications (scaling with N^2), leading to the demonstrable insight that for the considered scenario and typical N s and problem sizes the cost of gradient/expectation value evaluation will exceed that of evaluating the elementary propagators and their derivatives (scaling with N). To allow for efficiently optimising the reaction yield of radical pairs, we therefore suggest the adaptation of the gradient-based optimisation procedure as illustrated in Fig. 3.

First, we argue that the optimisation can be realised

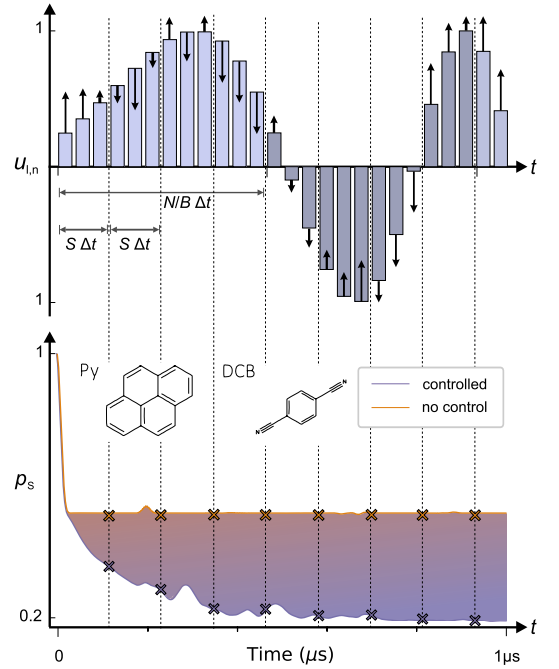


FIG. 3. Schematic illustration of the time-blocking and sparse-sampling approach used to reduce the computational expense of gradient-based optimisation of the radical pair recombination yield. The control amplitudes $u_{l,n}$ are simultaneously updated, whereby B disjoint blocks of $\frac{N}{B}$ time-steps each are considered in succession, with the initial state taken to be that of the system subject to the preceding optimised controls. A sparsely sampled approximation of the reaction yields based on $\frac{N}{BS}$ samples per block suffices to effectively optimise the reaction yield, in particular for larger spin systems for which the singlet probability is barely oscillatory. The bottom panel illustrates the unperturbed and minimised singlet probability for Py/DCB, an 18 spin exciplex system, driven by an RF control field of 0.1 mT in a static biasing field of 1 mT using 1024 control pulses of 1ns width, optimised using 256 samples of the singlet probability.

in practice in terms of B disjoint blocks of N/B timesteps each (time blocking). Second, we suggest that a sparsely sampled, i.e. crude, approximation of the reaction yield based on $N/(BS)$ samples per block, i.e. sampling every S th timestep, is also sufficient to adequately optimise the reaction yield. Here, B and S are integers that divide N and N/B , respectively. While this approach formally does not yield the optimum of the yield as formally defined in eq. (7), henceforth referred to as the complete optimum, we argue that, for suitably chosen B and S , yields optimised through sparsely sampled time blocking, realised at a fraction of computational effort, are sufficiently close to the true optimum. Third, to efficiently calculate the exponential propagators and the associated Fréchet derivatives, we use a scaling and squaring approach in combination with a Trotter-Suzuki splitting of the elementary propagator, as detailed in the Appendix. Lastly, to accelerate the optimisation we utilise L-BFGS-B, a limited memory variant of the Broyden-Fletcher-Goldfarb-Shanno algorithm, which preconditions gradients with curvature information in lieu of steepest descent [21].

A. Protocol applied to a prototypical spin system

We consider the minimisation of singlet recombination yield for a generalisation of the prototypical radical pair studied earlier in the work by Masuzawa et al. [18], where coherent control of a fidelity measure, rather than the reaction yield, was achieved in the simpler high-field scenario using time-local optimisation. Specifically, we assume a radical pair comprising 7 spin- $\frac{1}{2}$ particles, coupled through isotropic hyperfine (0.2, 0.5, 1 mT and 0.2 & 0.3 mT for the two radicals, respectively) and exchange interactions ($j_{ex}/(2\pi) = 1$ MHz), undergoing spin-selective recombination in the singlet state with rate constant $k_b = 1 \mu\text{s}^{-1}$ or spin independent escape with rate constant $k_f = 1 \mu\text{s}^{-1}$, such that $k_S = k_b + k_f$ and $k_T = k_f$. Given the high demand of completely optimising the seven-spin system, we have additionally studied the five-spin system resulting from the seven-spin system by retaining the three largest hyperfine coupling constants. Unlike Masuzawa et al. [18, 19], we seek to directly minimise the singlet recombination yield

$$Y_b = \frac{k_b}{k_b + k_f} Y_S \quad (27)$$

through a piece-wise constant control field applied perpendicular to a static biasing field, i.e. $L = 1$ and $V \equiv V_1 = \omega_1(\hat{S}_{1,x} + \hat{S}_{2,x})$, where ω_1 is the maximal Rabi frequency of the control field; control amplitudes are subject to $|u_{1,n}| \equiv |u_n| \leq 1$. We chose a discretisation time step of 1 ns and controlled the first $5 \mu\text{s}$ ($N = 5000$) after initialisation of the spin system in the singlet electronic state (thus accounting for more than 99.3% of radical decay; final yields still evaluated in the $t \rightarrow \infty \sim t_{max}$ limit with $t_{max} = 14 \mu\text{s}$). Fig. 4 illustrates exemplary

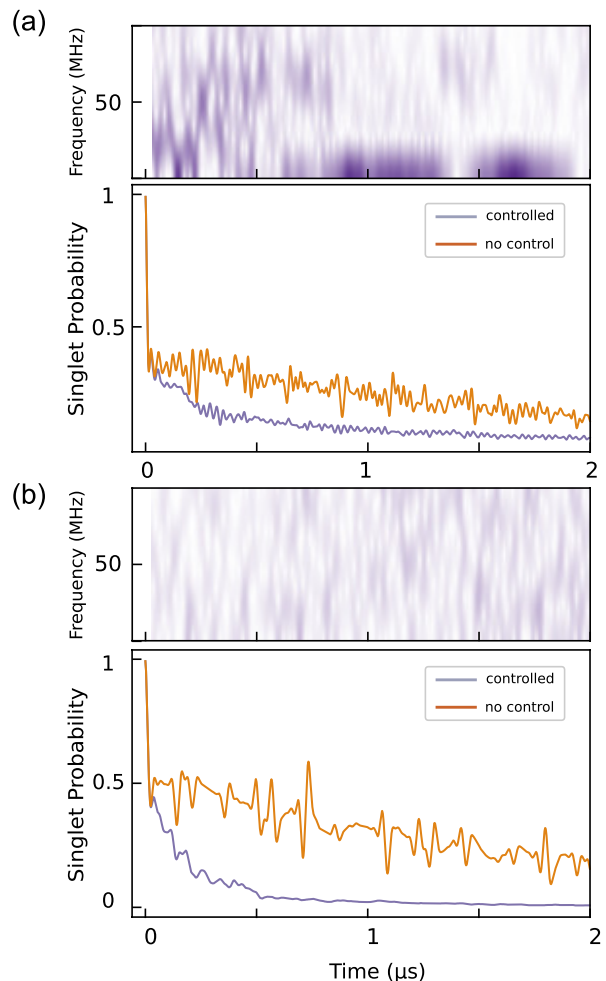


FIG. 4. Coherent control of the recombination dynamics for a 7 spin radical pair system under 0.5 mT and 10 mT static biasing field for (a) and (b), respectively. The recombination yield has been minimized for $N = 5000$ using $B = 2$ blocks of 2500 timesteps of 1 ns each, sparsely sampled using $S = 5$ or 10 for (a) and (b), respectively. The subfigures show the singlet probability, scaled to remove the spin-independent decay due to k_f , i.e. $\tilde{P}_S(t) \exp(k_f t)$, as a function of time after radical pair generation in the singlet state with (blue) and without (orange) control, below spectrograms of the control field magnitudes calculated using discrete Fourier transforms of 64 points, overlapped by 60 points and apodized using a Tukey window with shape parameter of 0.25. Using a control amplitude of 0.25 mT, the singlet recombination yield could be reduced to 0.156 (from 0.269 without control) and 0.097 (from 0.346) for the two biasing fields.

time dependent singlet probabilities, controlled and unperturbed, associated with this scenario for the biasing field intensities $B_0 = 0.5$ mT and 10 mT.

Efficient evaluation of single time-step propagators, and their Fréchet derivatives, was made possible via iterated Trotter-Suzuki splittings, and time blocking and sparse sampling of reaction yields, as introduced above. In view of Fig. 5 and comparable datasets for other biasing fields provided in the Supplemental Material (cf. Fig. S3), it is apparent that excellent control results can

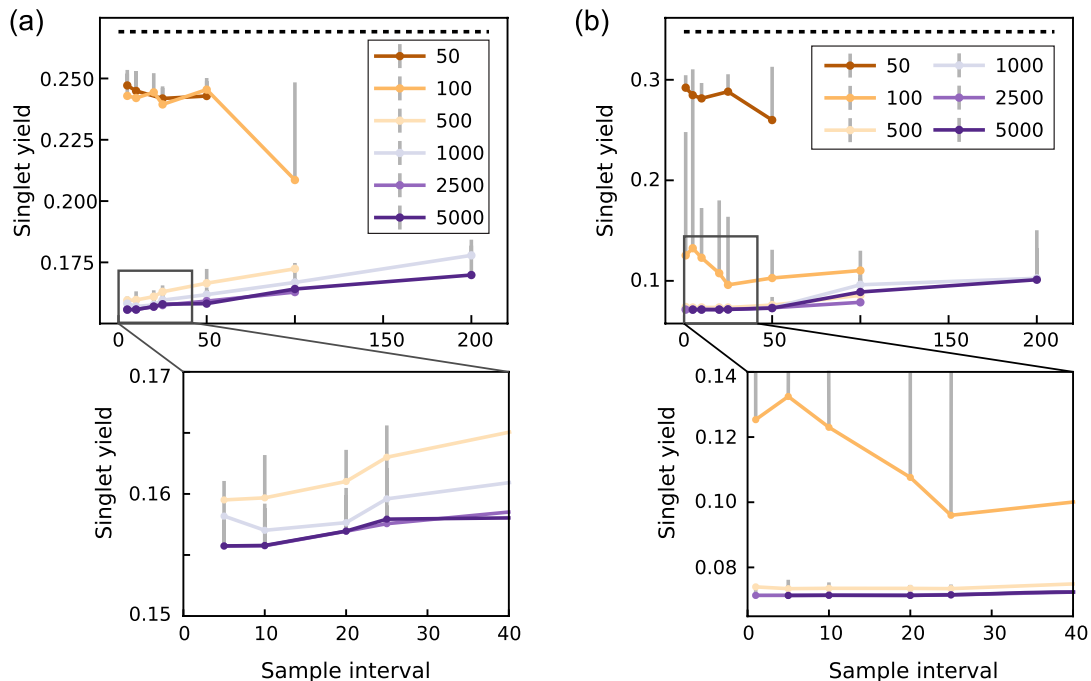


FIG. 5. For the seven and five-spin model systems, a maximal control field amplitude of 0.25 mT, with biasing fields of 0.5 and 10 mT for (a) and (b), respectively, we show singlet recombination yield as a function of S for yield minimisations using B blocks of N/B steps each, the latter value reported in the captions ($N = 5000$). The plots present the best minimisation result from 6 independent replications with randomly chosen initial control amplitudes (chosen from a normal random distribution truncated at ± 1); with dots indicate the 75-percentile range. The best optimisation results allowed a reduction of the singlet recombination yield from 0.269 to 0.156 and from 0.348 to 0.071 for (a) and (b), respectively.

be achieved for all N/B block sizes exceeding 500. Neither $B = 1$ and $N = B$ are strict necessities for practical control of the reaction outcome, substantially smaller blocks yield comparable optimisation results at a fractional cost. On the other hand, block sizes of 50 and 100 are unsatisfactory, indicating that a time-local optimisation is insufficient to yield optimal control results in the low to intermediate field region. For these inadequate block sizes, the optimisation result of the local BFGS optimisation algorithm is furthermore strongly dependent on the initial condition. Note that intermediate block sizes N/B are occasionally preferred over larger optimisation blocks, as the latter are less prone to get stuck in local minima, such that the overall optimisation outcome can be superior. This is, for example, seen in Fig. S3 for a biasing field of 1 mT, for which the best result of 6 replicated optimisations with $B = 2$ and $B = 5$ happened to surpass those with $B = 1$. Note furthermore that the optimisation results for smaller biasing fields, e.g. 0.5 mT, is more sensitive to the sampling interval, S , than for 10 mT. This is not surprising in view of the more varied singlet probability as a function of time observed for the lower field. This is encouraging insofar as more complex spin systems with diverse hyperfine interactions are expected to be less oscillatory. In any case, it appears that sampling intervals S of 25 and less are adequate here.

For the seven-spin system we found it impractical to re-

alise a complete set of optimisations for $S = 1$ and $B = 1$, i.e. complete, unblocked optimisation, as optimisation runs initiated from random configurations required more than a week to finish on the hardware utilised. However, a complete optimisation starting from the best blocked optimisation finished swiftly for the used tolerances without yielding a significant additional improvement. Furthermore, a single complete optimisation yielded results comparable to those of the good blocked and sparsely sampled optimisations. For the smaller 5-spin system, it is apparent that the sparsely sampled, blocked optimisations smoothly converge to the completely sampled optimum and that, again, $B > 1$ and $S > 1$ allow excellent practical optimisation outcomes relative to this (expensive) limit. See Fig. 5b and the Supplemental Material for these and further optimisation results achieved for the 5 and 7-spin systems in weak magnetic fields, including the geomagnetic field (cf. Fig. S1 and Fig. S2).

With the approach established, we set out to explore the prospects offered by controlling radical pair reaction yields in the weak to intermediate field case. Fig. 6a illustrates the results of minimising the singlet recombination yield as a function of the applied static magnetic field relative to the unperturbed scenario. These results were realised using 5 blocks of 1000 time steps of 1 ns and sampling the recombination yield from every 25th time point. The maximal control amplitude was 0.25 mT. The

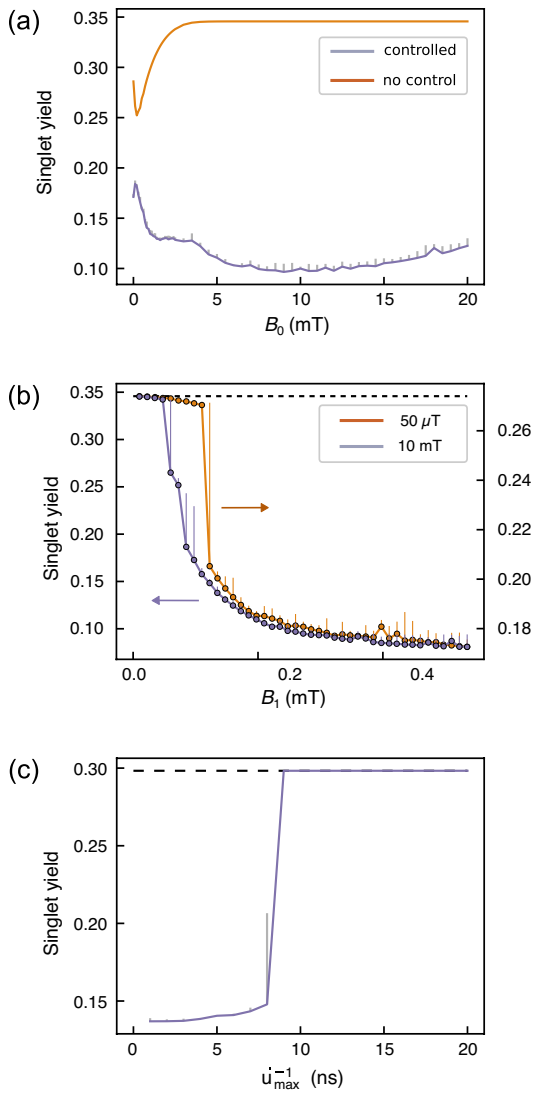


FIG. 6. Dependence on the optimisation outcome on the field strength of the biasing field and driving field, and the control speed for the 7-spin model system. In (a), we consider a 0.25 mT control field, and show yield minimisation against increasing B_0 (blue) in comparison to the un-controlled reference (orange). In (b) we show yield minimisation against increasing control field amplitude, B_1 , for a biasing field of $B_0 = 10$ mT and $50 \mu\text{T}$. In (c) we show the dependence of the singlet recombination yield at $B_0 = 1$ mT on the speed limit \dot{u}_{max}^{-1} . For all optimisations, $N = 5000$, $B = 5$ and $S = 25$.

plotted whiskers indicate 75-percentiles from 7 optimisations starting from random initial controls. Evidently, the recombination yield can be markedly reduced for all applied fields, the lowest yield realisable being 0.0966, realised for a biasing field of 9 mT. This amounts to a reduction by more than a factor of 3.5 compared to the uncontrolled yield at the same field (0.346). Generally, it is remarkable that the yields controlled for minimal recombination are all markedly lower than the minimal recombination yield of 0.252 realisable by applying a static magnetic field of 0.2 mT, i.e. the field matching the dip

in the singlet yield attributed to the low-field effect.

We have further analysed the dependence of the optimisation outcome on the strength of the control field. Fig. 6b shows Y_b as a function of the maximal control amplitude for the case of a static biasing field of 10 mT and $50 \mu\text{T}$, again realised by optimising 5 blocks of 1000 time steps, sampling every 25th. Appreciable minimisation for $B_0 = 10$ mT requires control amplitudes of 0.1 mT; controls with field strength below $\approx 50 \mu\text{T}$ do not elicit appreciable effects. This finding is in line with the well-studied effects of radio-frequency magnetic fields on radical pairs. In this scenario too, a resonant perturbation can only appreciably impact the spin evolution during the radical pair lifetime, τ , if $-\gamma B_1/(2\pi)\tau \gtrsim 1$, i.e. if the lifetime is sufficiently large to permit at least one Larmor precession in the field associate with the perturbation. As here $k_f^{-1} = 1 \mu\text{s}$ and $k_b^{-1} = 1 \mu\text{s}$, we can expect effects for B_1 exceeding $36 \mu\text{T}$ to $72 \mu\text{T}$ to become effective, which is in tentative agreement with the observed B_1 -dependence. On the other hand, driving fields larger than 0.1 mT allow very significant reductions of the recombination yield. It is interesting to note that for controlling reaction outcomes in the geomagnetic field ($B_0 = 50 \mu\text{T}$) slightly larger control fields exceeding 0.12 mT are required.

Above we have assumed that controls are applied with a time-resolution of $\Delta t = 1$ ns. While AWGs are available with sufficient sample rates and analog bandwidths (e.g. 50 GS/s at 15 GHz bandwidth) and the delivery of broadband magnetic fields at the required intensity has been realised (e.g. for high-field ENDOR spectroscopy [26]), the question of the minimal bandwidth to control radical pair reactions is a pertinent one. To this end, we have studied the dependence of the control result on the “speed limit” enforced on the control signal. Specifically, we stipulated that the controls must obey $|u_n - u_{n-1}| < \dot{u}_{max} \Delta t$. For $B_0 = 1$ mT, Fig. 6c summarizes the dependence of the singlet yield on this speed limit. We find that transition times of $\dot{u}_{max}^{-1} \gtrsim 8$ ns are required to elicit significant control; fast controls only deliver marginal additional gains. The minimal speed limit corresponds to a bandwidth of approximately $\frac{\dot{u}_{max}}{2} = 63$ MHz, which is of the order of, but smaller than, the magnitude of the spread of energy eigenvalues of the radical pair (93 MHz).

B. Protocol applied to a realistic exciplex-forming radical pair

We now present results for coherently controlling the symmetric recombination of a large spin system consisting of 18 spins. We consider the pyrene/para-dicyanobenzen (PY/DCB) exciplex-forming donor-acceptor systems in a solvent of moderate polarity [12, 27, 28]. The magnetosensitive, delayed fluorescence emission of this system has been widely studied. To make this large scale simulation tractable, we limit ourselves to

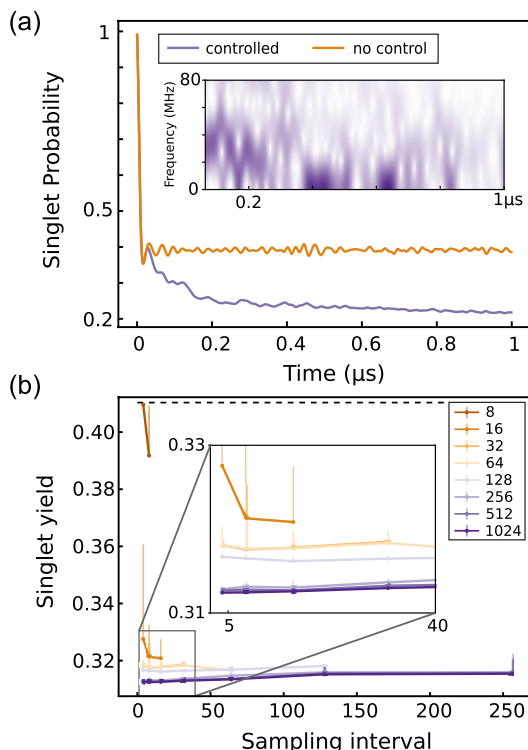


FIG. 7. Recombination yield minimisation of the 18 spin PY/DCB system in a bias field of 1 mT. (a) shows the singlet probability, scaled to remove the spin-independent decay due to k , i.e. $P_S(t) \exp(kt)$ with and without control. Control amplitudes were optimised using 32 samples and 1024 time-steps of 1 ns; a spectrogram of the control field magnitude is shown as insert. (b) shows the final yield as realized using l-BFGS complemented GRAPE for increasing sampling intervals and various block sizes, N/B , as indicated in the legend.

the scenario of homogeneous decay, i.e. $k_S = k_T = k$, and neglect inter-radical interactions. While this may appear crude at first glance, models typical of this have seen considerable success in the interpretation of experimental data [29]. The approximations are adequate since for the majority of its lifetime, the radical pair is in fact diffusively well separated, and the moderate reaction asymmetry of the real system (resulting from different electron transfer rate constants in the singlet and triplet state; the latter to the locally excited triplet state) has all but a small effect on the magnetic field sensitivity. Thus, in this limit, the singlet probability can be expressed as

$$\hat{P}_S(t) = e^{-kt} \left(\frac{1}{4} + \sum_{\alpha\beta \in \{x,y,z\}} R_{\alpha\beta}^{(1)}(t) R_{\alpha\beta}^{(2)}(t) \right), \quad (28)$$

where

$$\begin{aligned} R_{\alpha\beta}^{(i)}(t) &= \frac{1}{Z_i} \text{Tr} \left[\hat{S}_{i\alpha}(0) \hat{S}_{i\beta}(t) \right] \\ &= \frac{1}{Z_i} \text{Tr} \left[\hat{S}_{i\alpha} \hat{U}^\dagger(t, 0) \hat{S}_{i\beta} \hat{U}(t, 0) \right] \end{aligned} \quad (29)$$

are the electron spin correlation tensors for each spin in radical i , which are defined or calculable in the Hilbert

space of the individual radicals. Here, \hat{U} accounts for the coherent evolution only, i.e. $\hat{A}(T) = \hat{H}(T)$ (cf. eq. (6)). Thus, control of the radical pair reaction yield can be realised by separately calculating the gradients for each of the spin correlation tensors of two recombining radicals, and assembling the gradient of the reaction yield using the chain rule. Again, we follow the ideas of blocking the time axis and sparse sampling to increase the efficiency. In addition to the Trotter-Suzuki splitting discussed above, we use the fact that the Hamiltonian is only a function of the total nuclear spin associated with groups of completely equivalent spins, which permits an efficient calculation in the “coupled representation” [30]. Fig. 7 shows the minimisation of the PY/DCB singlet recombination yield for $k^{-1} = 200$ ns, a control amplitude of 0.2 mT, and a static basing field of 10 mT. The control was extended to the first 1024 time steps of 1 ns each. Varying block and sample sizes, again confirms practically sufficient fidelity from non-complete optimisation, as is demonstrated in Fig. 7b (also see Fig. S4).

IV. DISCUSSION

In electronic and nuclear spins of organic radical pairs, coherence lifetimes on the order of 100 ns to microseconds are typical, even in complex biological environments [31], opening a window of opportunity to realise control by applying time-dependent magnetic fields to manipulate reaction outcomes. Yet, the approach is still in its infancy. Experimental approaches have been limited to perturbing radical pair spin systems by radio-frequency magnetic fields [13, 17]. While positioned far from optimal control, these experiments are crucial as they demonstrate the principal possibility of influencing radical pair dynamics by RF-magnetic fields in weak magnetic fields. Examples of RF-magnetic field effects are furthermore well-established for biological radical pairs *in vivo* [13], such as those supposedly underpinning the avian compass sense. The latter are particularly noteworthy, because surprisingly weak RF-magnetic fields have been found to interrupt magnetoreception, suggesting an exquisitely sensitive underlying system of remarkable coherence time. Optimal quantum control protocols could be used to drive chemical and spin biological systems in a controlled and selective way, whereby reaction outcomes not attainable by static magnetic field perturbations alone become accessible. For quantum information processing in near term quantum hardware, among the many hurdles faced in counteracting environment-induced decoherence is the need to realise precise timing of quantum gate operations [32, 33] in nanosecond timescales. To evade this bottleneck, precise or adaptive [4, 34, 35] quantum control protocols may be harnessed to change the frequency of an applied control field dynamically throughout its pulse duration. But this is often hard to realise in practice, since formulating the appropriate optimal quantum control protocols is often highly non-trivial. In nature,

radical pairs seem to evade the effects of decoherence to retain exceptionally long coherence times, resulting in exquisite and unparalleled magnetometric sensitivity even in extremely noisy biological settings. Thus, optimal quantum control protocols, formulated with the primary aim of reproducing this sensitivity in spin-chemical reactions in solution, could also inform methods for similarly realising artificial or biological molecular [13, 36] qubits highly sensitive to applied magnetic fields. This could translate to further applications [32, 37–39] in both quantum metrology and quantum information processing. But to realise this goal, and future applications of optimal quantum control in a potentially biological context, efficient approaches for control design are vital.

The control of radical pair reactions is distinct from the majority of OQC approaches insofar as that the optimisation target is not defined at a particular instant of time, but encoded in the time-evolution from radical-pair creation to its eventual decay, $t \in [0, \infty)$, i.e. the reaction yield. Here, we have generalised the GRAPE-paradigm of using piecewise constant control amplitudes to realise reaction yield control. The suggested algorithm aims to overcome limitations of a previous approach by targeting actual reaction yields (rather than continuously updating the control to optimise a fidelity function involving observables that commute with the Hamiltonian or the singlet probability at one instance of time) and permitting control in weak magnetic fields. A time-global update scheme of control parameters (as opposed to the time-local approach from [18–20]), central to GRAPE, has here been found essential to realise the latter efficiently. The computational cost of optimisation of radical pair reaction yields by GRAPE has been viewed as prohibitive [18]. Significant costs are associated with the evaluation of numerous single time-step propagators and their Fréchet derivatives, and, for the optimisation of the reaction yields, in particular the calculation of the yield and its gradient through iterated matrix multiplications involving the former. Here, we have introduced a block-optimisation scheme and sparse sampling of the reaction yield to improve the efficiency of this step while retaining adequate control fidelity. To facilitate the efficient evaluation of propagators and their derivatives we have utilised an iterated Trotter-Suzuki splitting. We also exploit curvature information of the loss function in lieu of standard steepest decent/ascent approaches to reduce the number of optimisation steps required, as previously suggested [21]. These additional modifications we incorporate into the standard approach are vital for addressing the high computational costs, which had impeded earlier attempts to realise GRAPE-based reaction control of radical pair dynamics. We note that while sparse sampling of the reaction yield provides a useful, low-cost proxy to the actual reaction yield, we found that sampling of the singlet probability at one moment in time is often misleading the optimisation in weak magnetic field insofar as the increased/decreased probability at the chosen time does not necessarily correlate with increased/decreased

reaction yield. On the other hand, as we have shown, sparse sampling at a moderate sampling density reduces the computational cost while yielding close to optimal optimisation outcomes and a smooth progression for $B > 1$. We have further demonstrated the applicability of the approach as implemented here to realistically complex radical pair systems, such as the widely studied PY/DCB exciplex system subject to symmetric recombination.

The suggested approach can serve as a blueprint for future developments and optimisations. Although not explored here, some algorithmic modification could be tried, such as bottom-up strategies for which the sampling density is increased as the optimisation progresses. In addition, optimisation blocks could be overlapped. While here these approaches appeared unnecessary insofar as the suggested approach yielded control parameters that upon complete optimisation did not change significantly subject to the utilised termination criteria of the optimiser, these approaches could further speed up the rate at which this state is reached. Additional computational efficiency could furthermore be realised by reformulating the singlet yield evaluation in terms of the propagation of wave-packets, in particular in combination with using an incomplete basis for the nuclear spin functions and trace sampling [40]. We are currently developing such approaches with the aim of controlling the open system dynamics [41] of radical pairs. As for the calculation of propagators and derivatives, higher order operator splitting approaches could be used and the order of the approach, i.e. accuracy, to the optimisation process increased as the target function converges, as has been successfully demonstrated in [35] for a state transfer problem. Here, we have again refrained from these additional optimisations, as the generation of propagators and derivatives was not identified as the most time-consuming step for the considered problem sizes, which is related to the evaluation of reaction yields and gradients instead. From the reaction-control point of view, it is noteworthy that control has allowed us to suppress the singlet recombination to levels below those achievable by application of static magnetic fields of any strength. The achievable recombination yields are furthermore well-below the recombination yield of 25% expected to ensue for complete randomisation of the spin states. This shows that the control fields here do not merely enhance spin relaxation, as one might expect, but drive the system to optimal reaction outcomes.

We anticipate that optimal control of radical pair reactions will find applications in the context of biological radical pair reactions, either as an analytical tool or to drive the systems towards desired outcomes. For example, for biological radical pair reactions, such as those implicated with magnetoreception, a key problem to be addressed concerns distinguishing between different incarnations of radical reactions to better identify the underlying mechanism in a complex biological environment [42–44]. In this scenario, quantum control could allow us to derive control parameters that suppress magnetic

field effects in one mechanism while leaving those of alternative, competing models unaltered. Ultimately, control could allow us to turn MFEs into a tool to potentially control reaction processes of physiological relevance for applications in biology and medicine, by facilitating selective stimulation or suppression of cellular functions linked to radical pair processes. We hope that this work, by building on established techniques from quantum control like GRAPE to go beyond existing local optimisation methods, will lay the groundwork for realising this.

V. CONCLUSIONS

We have suggested and implemented a GRAPE-inspired approach to control reaction yields of radical pair recombination reactions through synchronised application of radio-frequency magnetic fields in a direction perpendicular to a static biasing field. We deviate from previous approaches by optimising reaction yields, i.e. the actual experimental observables, instead of fidelity measures defined at a particular time instants. Computational efficiency has been realised by block optimisation, sparse sampling, a split operator approach for calculating propagators and by utilising curvature information in the non-linear optimisation problem. The approach thus realised is applicable to radical pair systems of realistic complexity. We have demonstrated that control permits the reduction of the singlet recombination yield of a singlet-born model system to 10%, a yield unattainable by static magnetic field application alone, when using moderate control amplitudes and bandwidth (cf. Fig. 6). We hope that our approach helps accelerate the adoption of control approaches for radical pair recombination reactions in low external fields. We anticipate that these future applications will utilise control beyond mere reaction control, for example to realise distinguishability of radical pairs in complex environments and for facilitating model selection for competing hypothesis based on experiments with optimised contrast power.

APPENDIX

A. Sparse Blocking

The control of reaction yields via numerical approaches like GRAPE is expected to be costly. The computational demand is particularly large if, as we do here (and unlike [18, 19]), the goal is to optimise yields of radical pair reactions, which are time-integral quantities (cf. eq. (7)); unlike the typical fidelity measures in quantum control applications pertaining to the implementation of a state transfer or a unitary operation for a fixed time t). The approach requires repeated matrix multiplications for evaluating the time-dependent singlet-probabilities that sum to the recombination yield (and its associated gra-

dients). Formally, eq. (25) implies

$$\sum_{n=1}^N [(n-1) + 3] + nL[(n-1) + 3] = O(N^3) \quad (\text{A1})$$

matrix multiplications (i.e. for every t_n , $(n-1)$ matrix multiplications are required to evaluate \hat{U} , $(n-1)$ to evaluate $\hat{U}_+ \hat{W}_{n,l} \hat{U}_-$ (via $L_{n,l}$) for every l and n ; and an additional three each to evaluate the expectation value/gradients). In practical implementations, the estimate in eq. (A1) can be improved upon by preserving terms from previous n , i.e. $n-1$. allowing the update of \hat{U} and $\hat{U}_+ \hat{W}_{n,l} \hat{U}_-$ with a singular matrix multiplication (instead of $n-1$), thus requiring

$$\sum_{n=1}^N 4(1 + nL) = 2LN^2 + 2(L+2)N \quad (\text{A2})$$

matrix multiplications. Nevertheless, due to the quadratic scaling of the evaluation of eq. (26) with N , the gradient/expectation value evaluation will often exceed the cost of evaluating the elementary propagators and their derivatives (scaling as N) for large N and thus be the limiting factor. To efficiently optimise the reaction yield of complex radical pairs, we suggest the following adaptation of the gradient-based optimisation procedure. We postulate that the optimisation can be realised in terms of B disjoint blocks of N/B time-steps each (time blocking), with the initial state taken as that of the system subject to the preceding optimised controls, sparsely sampled using $N/(BS)$ samples per block, as illustrated in Fig. 3. Here, B and S are integers that divide N and B , respectively. The number of matrix multiplications in this approach is reduced to

$$\begin{aligned} & B \left(\sum_{n=1}^{N/B} (1 + nL)[1 + 3(\delta_{n \bmod s, 0})] \right) \\ &= B \left(\sum_{n=1}^{N/B} (1 + nL) + 3 \sum_{m=1}^{N/BS} (1 + LS) \right) \\ &= \frac{N^2 L(S+3)}{2BS} + N \left(2L + 1 + \frac{3}{S} \right). \end{aligned} \quad (\text{A3})$$

The number of matrix multiplications necessary in general still scales quadratically with N , i.e. as $O(N^2/B)$. Linear scaling is only obtained in the limit that $B = N$, i.e. time-local optimisation. But in practice, the block size can be chosen much smaller than N , i.e. $N/B \ll N$, to realise a substantial speedup, whilst delivering adequate practical optimisation of the reaction yield. Furthermore, for $S \gg 3$, the complexity of the algorithm approaches independence of S .

B. Trotter-Suzuki Splitting

To efficiently calculate the propagators and the associates Fréchet derivatives, we use a scaling and squaring approach in combination with a Trotter-Suzuki splitting of the elementary propagator. Specifically, we compute the matrix exponent

$$e^X = \left(e^{2^{-s} X} \right)^{2^s} \quad (\text{A4})$$

by $s \in \mathbb{N}$ repeated squaring starting from $e^{2^{-s}X}$ calculated as

$$e^{2^{-s}X} = e^{-i2^{-s-1}\Delta t \hat{A}'} e^{-i2^{-s}\Delta t \hat{A}''} e^{-i2^{-s-1}\Delta t \hat{A}'} + O\left(\frac{\Delta t^2}{2^{2s}}\right),$$

with

$$X = -i\hat{A}'dt - i\hat{A}''dt \quad (\text{A5})$$

being a convenient splitting of $X = -idt\hat{A}_i$ (cf. eq. (18)). Practically, \hat{A}' and \hat{A}'' represent the drift and control Hamiltonians respectively. If the latter is based on coupling applied magnetic fields via the Zeeman interaction, the propagator under \hat{A}'' can be expressed as a direct product of evolution operators for the individual electron spins based on expression

$$e^{-i\omega\hat{n}\cdot S} = \cos\left(\frac{\omega}{2}\right)I - 2i\sin\left(\frac{\omega}{2}\right)\hat{n}\cdot S \quad (\text{A6})$$

where $\omega \in \mathbb{N}$ is a parameter related to the strength of the control field and n in a unit vector specifying the orientation of the perturbation in the laboratory frame.

Likewise, the Fréchet derivative of the exponential e^X can be evaluated using an s -fold recurrence, based on [45]

$$L(X, E) = e^{X/2}L(X/2, E/2) + L(X/2, E/2)e^{X/2} \quad (\text{A7})$$

obtained by differentiating $e^X = (e^{X/2})^2$ using the chain rule. In combination with eq. (A4), the only derivatives that are explicitly required in this processes are those of $e^{-i2^{-s}\Delta t \hat{A}''}$. For Zeeman coupling with a single-spin propagator as given by eq. (A6), the necessary Fréchet derivatives can be obtained in analytic form, in combination with the chain rule, from

$$L(\omega\hat{n}\cdot S, -i\hat{n}\cdot S) = -i\cos\left(\frac{\omega}{2}\right)\hat{n}\cdot S - \frac{1}{2}\sin\left(\frac{\omega}{2}\right)\mathbb{1}. \quad (\text{A8})$$

We optimised using the limited memory variant of the Broyden–Fletcher–Goldfarb–Shanno (l-BFGS) algorithm, which preconditions gradients using curvature information, and used the implementation available in SciPy [46] with a stopping criterion of 10^{-6} and 10^{-7} for the change of the sparsely sampled yield and the projected gradient, respectively. The maximum number of iterations was set to 200. We further ran simulations in parallel for varying number of blocks B and the sampling interval S , as seen in Figs. 5(a) and 5(b), to assess the performance and scalability of our approach.

ACKNOWLEDGMENTS

This work was supported by the Office of Naval Research (ONR Award Number N62909-21-1-2018). We acknowledge use of University of Exeter’s HPC facility.

-
- [1] Koch et al. Quantum Optimal Control in Quantum Technologies. Strategic report on current status, visions and goals for research in Europe. *EPJ Quantum Technol.*, 9(1):19, 2022.
- [2] David J. Tannor, Ronnie Kosloff, and Stuart A. Rice. Coherent pulse sequence induced control of selectivity of reactions: Exact quantum mechanical calculations. *J. Chem. Phys.*, 85(10):5805–5820, 1986.
- [3] David J. Tannor and Stuart A. Rice. Control of selectivity of chemical reaction via control of wave packet evolution. *J. Chem. Phys.*, 83(10):5013–5018, 1985.
- [4] Tobias Brixner and Gustav Gerber. Quantum control of gas-phase and liquid-phase femtochemistry. *Chem. Phys. Chem.*, 4(5):418–438, 2003.
- [5] Jonathan P. Dowling and Gerard J. Milburn. Quantum Technology: The Second Quantum Revolution. *Philos. Trans. R. Soc. A*, 361(1809):1655–1674, 2003.
- [6] Blanka Pophof, Bernd Henschenmacher, Daniel R. Kattnig, Jens Kuhne, Alain Vian, and Gunde Ziegelberger. Biological effects of electric, magnetic, and electromagnetic fields from 0 to 100 mhz on fauna and flora: Workshop report. *Health Phys.*, 124:39–52, 2023.
- [7] Blanka Pophof, Bernd Henschenmacher, Daniel R. Kattnig, Jens Kuhne, Alain Vian, and Gunde Ziegelberger. Biological effects of radiofrequency electromagnetic fields above 100 mhz on fauna and flora: Workshop report. *Health Phys.*, 124:31–38, 2023.
- [8] Michael R. Wasielewski, Christian H. Bock, Michael K. Bowman, and James R. Norris. Controlling the duration of photosynthetic charge separation with microwave radiation. *Nature*, 303(5917):520–522, 1983.
- [9] Kevin B. Henbest, Philipp Kukura, Christopher T. Rodgers, P. J. Hore, and Christiane R. Timmel. Radio frequency magnetic field effects on a radical recombination reaction: A diagnostic test for the radical pair mechanism. *J. Am. Chem. Soc.*, 126(26):8102–8103, 2004.
- [10] Christopher T. Rodgers, C. J. Wedge, Stuart A. Norman, Philipp Kukura, Karen Nelson, Neville Baker, Kiminori Maeda, Kevin B. Henbest, P. J. Hore, and C. R. Timmel. Radiofrequency polarization effects in zero-field electron paramagnetic resonance. *Phys. Chem. Chem. Phys.*, 11:6569–6572, 2009.
- [11] C. J. Wedge, Christopher T. Rodgers, Stuart A. Norman, Neville Baker, Kiminori Maeda, Kevin B. Henbest, C. R. Timmel, and P. J. Hore. Radiofrequency polarization effects in low-field electron paramagnetic resonance. *Phys. Chem. Chem. Phys.*, 11(31):6573–6579, 2009.
- [12] G. Grampp, M. Justinek, and S. Landgraf. Magnetic field effects on the pyrene—dicyanobenzene system: determination of electron self-exchange rates by many spectroscopy. *Mol. Phys.*, 100(8):1063–1070, 2002.
- [13] Tomoyasu Mani. Molecular qubits based on photogenerated spin-correlated radical pairs for quantum sensing. *Chem. Phys. Rev.*, 3(2):021301, 2022.
- [14] Daniel R. Kattnig. F-cluster: Reaction-induced spin correlation in multi-radical systems. *J. Chem. Phys.*, 154(20):204105, 2021.
- [15] P. J. Hore and Henrik Mouritsen. The radical-pair mechanism of magnetoreception. *Annu. Rev. Biophys.*, 45:299–344, 2016.
- [16] Thorsten Ritz, Roswitha Wiltschko, P. J. Hore, Christopher T. Rodgers, Katrin Stapput, Peter Thalau, Christiane R. Timmel, and Wolfgang Wiltschko. Magnetic compass of birds is based on a molecule with optimal

- directional sensitivity. *Biophys. J.*, 96:3451–7, 2009.
- [17] Svenja Engels, Nils-Lasse Schneider, Nele Lefeldt, Christine Maira Hein, Manuela Zapka, Andreas Michalik, Dana Elbers, Achim Kittel, P. J. Hore, and Henrik Mouritsen. Anthropogenic electromagnetic noise disrupts magnetic compass orientation in a migratory bird. *Nature*, 509:353–6, 2014.
- [18] K. Masuzawa, M. Sato, M. Sugawara, and Kiminori Maeda. Quantum Control of Radical Pair Reactions by Local Optimization Theory. *J. Chem. Phys.*, 152:014301, 2020.
- [19] A. Tateno, K. Masuzawa, H. Nagashima, and Kiminori Maeda. Anisotropic and Coherent Control of Radical Pairs by Optimized RF Fields. *Int J Mol Sci.*, 24(11):9700, 2023.
- [20] M. Sugawara. General formulation of locally designed coherent control theory for quantum system. *J. Chem. Phys.*, 118(15):6784–6800, 2003.
- [21] P. de Fouquieres, S.G. Schirmer, S.J. Glaser, and Ilya Kuprov. Second order gradient ascent pulse engineering. *J. Magn. Reson.*, 212(2):412–417, 2011.
- [22] Erik M. Gauger, Elisabeth Rieper, John J. L. Morton, Simon C. Benjamin, and Vlatko Vedral. Sustained quantum coherence and entanglement in the avian compass. *Phys. Rev. Lett.*, 106:040503, 2011.
- [23] S. Machnes, U. Sander, S. J. Glaser, P. de Fouquieres, A. Gruslys, S. Schirmer, and T. Schulte-Herbrüggen. Comparing, optimizing, and benchmarking quantum-control algorithms in a unifying programming framework. *Phys. Rev. A*, 84:022305, 2011.
- [24] Navin Khaneja, Timo Reiss, Cindie Kehlet, Thomas Schulte-Herbrüggen, and Steffen J Glaser. Optimal control of coupled spin dynamics: design of NMR pulse sequences by gradient ascent algorithms. *J. Magn. Reson.*, 172(2):296–305, 2005.
- [25] R. M. Wilcox. Exponential Operators and Parameter Differentiation in Quantum Physics. *J. Math. Phys.*, 8:962–982, 1967.
- [26] M. M. Hertel, V. P. Denysenkov, M. Bennati, and T. F. Prisner. Pulsed 180-ghz epr/endor/peldor spectroscopy. *Magn. Reson. Chem.*, 43(S1):S248–S255, 2005.
- [27] Daniel R. Kattnig, Arnulf Rosspeintner, and Günter Grampp. Magnetic field effects on exciplex-forming systems: the effect on the locally excited fluorophore and its dependence on free energy. *Phys. Chem. Chem. Phys.*, 13:3446–3460, 2011.
- [28] Hao Minh Hoang, Thi Bich Van Pham, Günter Grampp, and Daniel R. Kattnig. Exciplexes versus loose ion pairs: How does the driving force impact the initial product ratio of photoinduced charge separation reactions? *J. Phys. Chem. Lett.*, 5(18):3188–3194, 2014.
- [29] Hisaharu Hayashi. *Introduction to Dynamic Spin Chemistry: Magnetic Field Effects on Chemical and Biochemical Reactions*. Vol. 8 in World Scientific Lecture and Course Notes in Chemistry. World Scientific Publishing Company, 2004.
- [30] Chadsley Atkins, Kieran Bajpai, Jeremy Rumball, and Daniel R. Kattnig. On the optimal relative orientation of radicals in the cryptochrome magnetic compass. *J. Chem. Phys.*, 151(6):065103, 2019.
- [31] Daniel R. Kattnig, Ilia A. Solov'yov, and P. J. Hore. Electron spin relaxation in cryptochrome-based magnetoreception. *Phys. Chem. Chem. Phys.*, 18:12443–12456, 2016.
- [32] Haochuan Mao, Gediminas J. Pažėra, Ryan M. Young, Matthew D. Krzyaniak, and Michael R. Wasielewski. Quantum gate operations on a spectrally addressable photogenerated molecular electron spin-qubit pair. *J. Am. Chem. Soc.*, 145(11):6585–6593, 2023.
- [33] Jake Xuereb, Paul Erker, Florian Meier, Mark T. Mitchison, and Marcus Huber. The impact of imperfect time-keeping on quantum control. *arXiv*, 2023.
- [34] T Brixner and G Gerber. Adaptive quantum control of femtochemistry. *Phys. Scr.*, 2004(T110):101, 2004.
- [35] David L. Goodwin, Pranav Singh, and Mohammadali Foroozandeh. Adaptive optimal control of entangled qubits. *Sci. Adv.*, 8(49):eabq4244, 2022.
- [36] Wasielewski et al. Exploiting chemistry and molecular systems for quantum information science. *Nat. Rev. Chem.*, 4(9):490–504, 2020.
- [37] Jianming Cai, Gian Giacomo Guerreschi, and Hans J. Briegel. Quantum control and entanglement in a chemical compass. *Phys. Rev. Lett.*, 104:220502, 2010.
- [38] Jia-Yi Wu, Xin-Yuan Hu, Hai-Yuan Zhu, Ru-Qiong Deng, and Qing Ai. A Bionic compass based on Multiradicals. *J. Phys. Chem. B*, 126(49):10327–10334, 2022.
- [39] Ziyuan Li, Huapeng Yu, Tongsheng Shen, Ye Li, and Wenjun Zhang. Bionic Magnetic Compass Algorithm Based on Radical Pair Theory. *IEEE Sens.*, 22(24):23812–23820, 2022.
- [40] Thomas P. Fay, Lachlan P. Lindoy, and David E. Manolopoulos. Spin relaxation in radical pairs from the Stochastic Schrödinger equation. *J. Chem. Phys.*, 154:084121, 2021.
- [41] Shimshon Kallush, Roie Dann, and Ronnie Kosloff. Controlling the uncontrollable: Quantum control of open-system dynamics. *Sci. Adv.*, 8(44):eadd0828, 2022.
- [42] H. G. Hiscock, T. W. Hiscock, D. R. Kattnig, T. Scrivener, A. M. Lewis, D. E. Manolopoulos, and P. J. Hore. Navigating at night: fundamental limits on the sensitivity of radical pair magnetoreception under dim light. *Q. Rev. Biophys.*, 52:e9, 2019.
- [43] Amit Finkler and Durga Dasari. Quantum sensing and control of spin-state dynamics in the radical-pair mechanism. *Phys. Rev. Applied*, 15:034066, 2021.
- [44] Xu et al. Magnetic Sensitivity of Cryptochrome 4 From a Migratory Songbird. *Nature*, 594(7864):535–540, 2021.
- [45] Awad H. Al-Mohy and Nicholas J. Higham. Computing the fréchet derivative of the matrix exponential, with an application to condition number estimation. *SIAM J. Matrix Anal. Appl.*, 30(4):1639–1657, 2009.
- [46] Virtanen et al. and SciPy 1.0 Contributors. SciPy 1.0: Fundamental Algorithms for Scientific Computing in Python. *Nat. Methods*, 17:261–272, 2020.

Supplemental Material

Quantum Control of Radical Pair Dynamics beyond Time-local Optimisation

Farhan T. Chowdhury, Matthew C. Denton, Daniel C. Bonser, and Daniel R. Kattnig*

Department of Physics and Living Systems Institute

University of Exeter, Stocker Road, Exeter, Devon, EX4 4QD, United Kingdom

E-mail: d.r.kattnig@exeter.ac.uk

We provide further results for the minimisation of the recombination yield of the 5-spin system in the low-magnetic field regime, including the geomagnetic field. This is followed by additional results for the 5-spin systems controlled under $100 \mu\text{T}$, with and without a speed limit imposed. To further support the case for global optimisation over time-local methods, which roughly correspond to what is achievable with GRAPE for insufficient block sizes, we further present plots for 5-spin systems showing singlet recombination yields as a function of S for yield minimisations using B blocks of N/B steps each. Finally, an additional figure shows the frequency profile and recombination yields realized using l-BFGS complemented GRAPE for increasing sample intervals for the 18 spin PY/DCB system driven by an RF control field of 0.1 mT.

TABLE I. Dependence of the optimized recombination yield and runtime of the BFGS algorithm, as implemented in `scipy.optimize.minimize`, on the tolerancy `ftol`. 15 attempts to minimize the recombination yield of the 7-spin model system starting from random initial states uniformly distributed in $[-1, 1]$ were recorded. The biasing field amounted to 1 mT and the maximal control field amplitude to 0.25 mT. The minimal yield realized was 0.1336. The iterative algorithm stops when $(f^k - f^{k+1})/\max(|f^k|, |f^{k+1}|, 1) \leq ftol$, where f^k is the sparse approximation of the yield at iteration k . For the application considered here, the denominator equals 1. $N = 5000$, $B = 5$, $S = 200$.

ftol	Recombination Yield (minimal)	Recombination Yield (average)	runtime (s)
4	0.2665	0.2738 ± 0.0039	75.6 ± 0.8
4.5	0.1354	0.1496 ± 0.0367	1522 ± 480
5	0.1345	0.1376 ± 0.0019	2132 ± 298
6	0.1343	0.1374 ± 0.0022	6483 ± 543
7	0.1338	0.1375 ± 0.0022	8886 ± 447
8	0.1336	0.1372 ± 0.0020	9959 ± 113

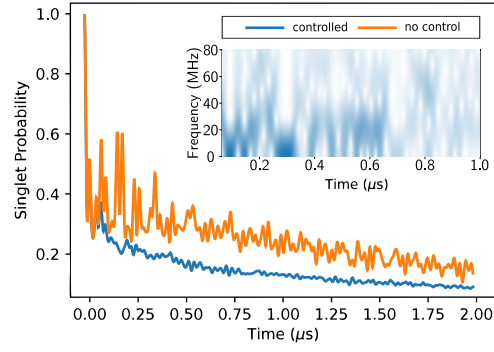


FIG. S1. Using GRAPE to control the 5-proton spin system in the geomagnetic field ($50 \mu\text{T}$), with the singlet probability optimised over 5000 time-steps of 1 ns using 2 cycles of 2500 time-steps and 250 sampling points. The control amplitude amounted to 0.25 mT.

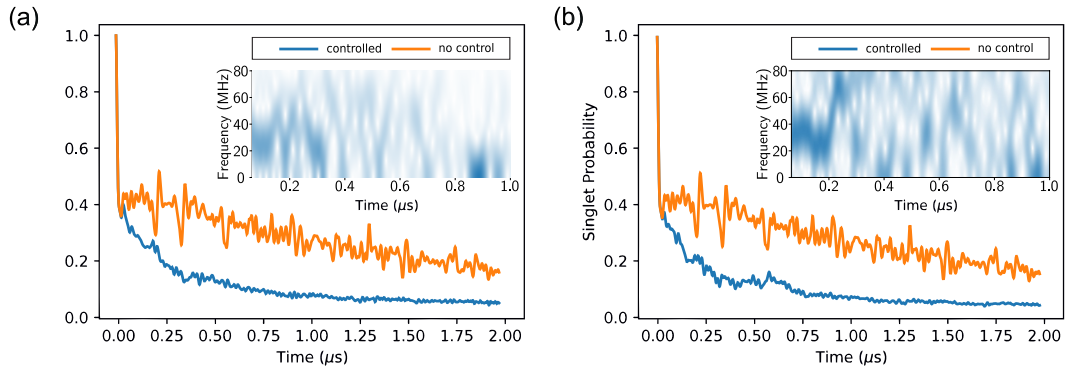


FIG. S2. Using GRAPE to control the 5-proton spin system under $100 \mu\text{T}$ magnetic field, subject to a speed limit of $\dot{u}_{max} = 0.2 \text{ ns}^{-1}$ in (a), and without in (b), with the singlet probability optimised using 2 cycles of 2500 time-steps and 250 sampling points.

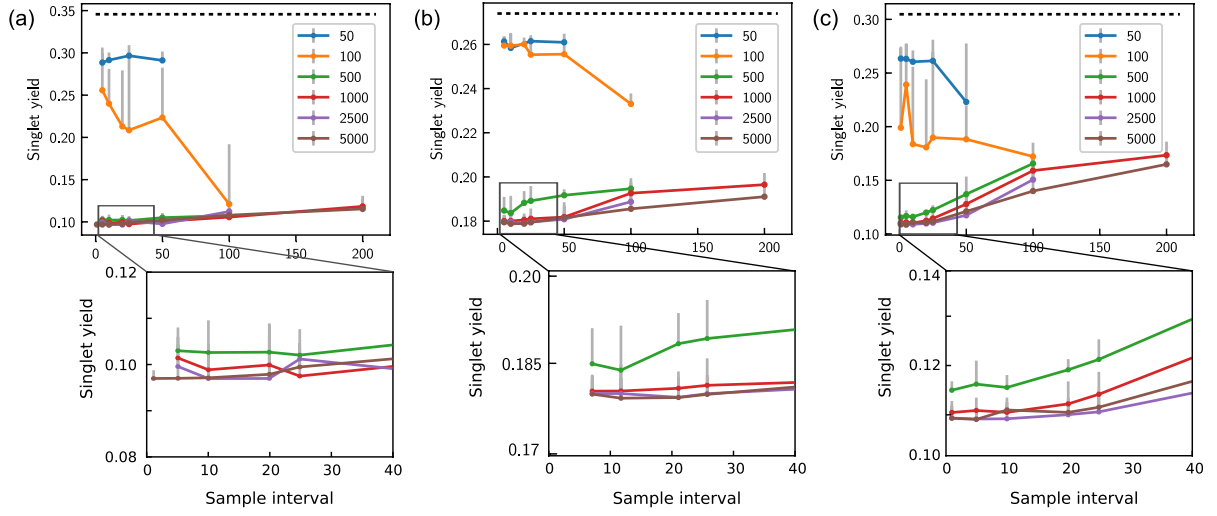


FIG. S3. For 5-proton and 3-proton model systems in (a)-(b) and (c), respectively, with a maximal control field amplitude of 0.25 mT , with biasing fields of $50 \mu\text{T}$, 10 mT and 1 mT for (a), (b) and (c), respectively, we show singlet recombination yield as a function of S for yield minimisations using B blocks of N/B steps each.

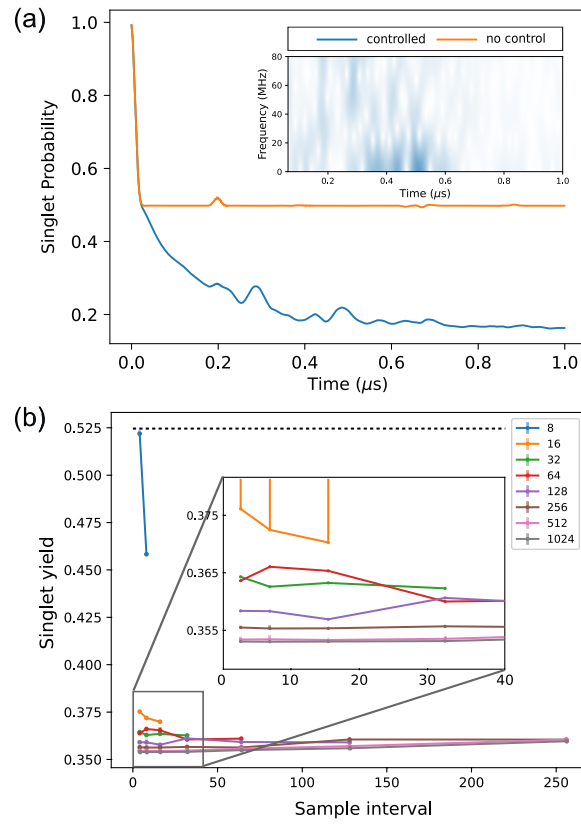


FIG. S4. We show the frequency profile and recombination yield minimisation using l-BFGS complemented GRAPE for increasing sample intervals for the 18 spin PY/DCB system, driven by an RF control field of 0.1 mT in a static biasing field of 1 mT using 1024 control pulses of 1 ns width.